IEEE Access
Multidisciplinary ⋮ Rapid Review ⋮ Open Access Journal

Received 30 August 2023, accepted 17 September 2023, date of publication 20 September 2023,
date of current version 27 September 2023.

Digital Object Identifier 10.1109/ACCESS.2023.3317511

RESEARCH ARTICLE

A Reflective Metalens With Tunable Focal Length for Millimeter Waves

MOHAMMAD ALI SHAMELI[1], MIRKO MAGAROTTO[1], (Member, IEEE), ANTONIO-D CAPOBIANCO[1,3], (Member, IEEE), LUCA SCHENATO[1,3], (Member, IEEE), MARCO SANTAGIUSTINA[1,3], (Member, IEEE), AND DOMENICO DE CEGLIA[2,3,4], (Member, IEEE)

[1]Department of Information Engineering, University of Padova, 35131 Padua, Italy
[2]Department of Information Engineering, University of Brescia, 25123 Brescia, Italy
[3]National Inter-University Consortium for Telecommunications (CNIT), 43124 Parma, Italy
[4]National Institute of Optics—National Research Council, 25123 Brescia, Italy

Corresponding author: Mohammad Ali Shameli (Mohammadali.shameli@unipd.it)

This work was supported in part by the European Union under the Italian National Recovery and Resilience Plan (NRRP) of NextGenerationEU, Partnership on "Telecommunications of the Future" under Grant PE0000001-program "RESTART;" in part by the University of Padova under Grant SEED-BIRD2020; and in part by Italian Ministry for Education, Universities and Research [Ministero dell'Istruzione, dell'Università e della Ricerca (MIUR)] under Grant PRIN 2017HP5KH7_003-FIRST.

ABSTRACT A novel architecture of reconfigurable, flat metalens is proposed with an electrically tunable focal length for applications in wireless communication systems working at the frequencies of millimeter waves (i.e., 60 GHz). In this approach, a reflective metalens made of silicon bricks is distributed on a grounded multilayer hosting films of a phase-transition material, namely, vanadium dioxide. The multilayer, acting as a ground plane with a controllable position, provides different phase profiles in the same metalens and, therefore, different focal lengths. Our numerical investigation of thermal and electromagnetic effects shows that the metasurface can reversibly tune the focal length at 27, 31, and 33 mm. In addition, in the operating frequency range between 58 and 62 GHz, the tunability of the metalens remains unaltered. Dynamically controlling the focal point of millimeter waves is highly desirable in wireless communications, especially for 5G and 6G cellular systems applications.

INDEX TERMS Millimeter waves, tunable and active metasurfaces, reconfigurable devices, reflective metalens, vanadium dioxide.

I. INTRODUCTION

Nowadays, a considerable increase in wireless consumers and a growing need for wide spectrum bandwidth with a higher data rate have forced engineers and researchers to transition from microwaves to millimeter waves [1], [2], [3]. Millimeter waves provide large bandwidth, narrow beams, and strong detection ability, while most wireless systems at microwave frequencies present smaller data rates [1], [2], [3]. In other words, millimeter waves with a spectrum between 30 GHz and 300 GHz and devices with a smaller footprint compared to microwave structures are reliable alternatives for future wireless communications [1], [2]. Fifth-generation (5G) and sixth-generation (6G) cellular communication systems with improved quality and limited-service power are the most prominent applications of millimeter waves [4], [5], [6]. Future wireless systems based on millimeter waves will provide larger bandwidth, improved spectrum efficiency, giga-bit per second data rate, and low latency [4], [5], [6].

Medical applications are another significant field of millimeter waves [7], [8]. For example, medical imaging with millimeter waves provides superior resolution with respect to microwaves; additionally, compared to X-rays, millimeter waves are safer and do not require expensive and advanced fabrication techniques [7]. Another application in medicine is the contactless measurement of arterial pulses, which can be used in pulse analysis and measurement, especially for blood pressure tracking [8].

The associate editor coordinating the review of this manuscript and approving it for publication was Wanchen Yang.

The development of technologies that rely on millimeter waves requires the realization of several devices able to radiate, receive, and control such frequencies. Furthermore, devices with reconfigurability and fast tuning of the electromagnetic response are essential features for high-data-rate wireless communication systems. In particular, there is a need for intelligent wireless communication systems composed of reconfigurable and smart devices able to direct power in desired directions while maintaining a high degree of directivity. In other words, the use of intelligent structures such as metasurfaces, thanks to their field manipulation capabilities, achieved through low-cost, lightweight, and planar structures, is able to control the propagation of electromagnetic (EM) waves to prevent the detrimental effects included by the environment, such as fading, clutter, and blockage, which is inevitable in wireless communication systems, especially in millimeter waves [9]. Also, controlling the wavefront, frequency, and even polarization of the impinging signals realized by this kind of structure frees us from complex decoding and encoding [10], and the dispersion characteristics of meta-atoms proposed by [11] can realize a metasurface with these capabilities. So far, few reconfigurable devices have been demonstrated for millimeter waves, including a frequency-reconfigurable metasurface antenna [12] and a reconfigurable metasurface beam steering [13] exploiting vanadium dioxide (VO_2). The digital metasurface of [14] can steer a beam by tuning a DC-bias voltage applied to nematic liquid crystals (NLCs). A reconfigurable antenna with a tunable radiation pattern is realized with a switch p-i-n diode in [15]. Despite these efforts, a flat reconfigurable lens with the capability to tune the focal length is extremely challenging to achieve, not only in the millimeter-waves range but also in different portions of the electromagnetic spectrum since each focal point location requires a different nonlinear phase profile. Changing the spherical wave to the plane wave and vice versa is one of the significant applications of using a tunable lens in millimeter waves, especially when the electromagnetic wave direction changes, which is inevitable in this frequency range [16]. Imaging [17], detection [18], and security [19] are the other applications for such tunable lenses in the millimeter wave regime.

Reconfigurability of the electromagnetic response of metasurfaces may be achieved through different active approaches, including 4-N, N-dimethylamino-4'-N'-methylstilbazolium tosylate (DAST) as optoelectronic materials with DC bias voltage [20], or altering the density of the carriers in conductive oxides such as indium-tin-oxide (ITO) [21]. Phase transition materials (PTMs) such as liquid crystals can significantly modify the electromagnetic response of devices by using an external bias to control the refractive index [22]. Additionally, Sb_2S_3 [23], Sb_2Se_3 [24], $Ge_2Sb_2Te_5$ (GST) [25], and $Ge_2Sb_2Se_4Te_1$ (GSST) [26], which display inherently non-volatile phase transitions, can be used to regulate the performance of structures by electrical, optical, or thermal stimuli. The digital coding metasurface is a novel reconfigurable structure in microwave frequency to control propagation direction and harmonic power distribution simultaneously, which is controlled by a field-programmable gate array [27]. Another work proposed reconfigurable anisotropy and functional transformation with a thin film resistor and VO_2 that can change between a truncated cloak and concentrator upon external temperature change [28]. Despite the ability of these materials to provide reconfigurability of devices, lack of feasibility [20], low operational speed in the millimeter-wave range [22], [29], and low performance in comparison with optical frequency [22], [23], [24], [25], [26] restrict their use in the development of high-speed reconfigurable metasurfaces at millimeter waves. To address these significant challenges, we propose the use of VO_2, one of the most attractive and high-speed phase transition materials [24], that can be reversibly switched between a high-resistance insulator phase and a low-resistance metallic phase at a critical temperature of $T_c = 68$ °C. This switching can be activated by light, direct heating, or electrical stimuli. Additionally, VO_2 is considered the most promising thermochromic material in terms of stability and commercialization due to its cost efficiency and performance in the regime of millimeter waves [12], [13].

Lenses with tunable focal lengths have been investigated using different active materials and a variety of configurations. In the microwave regime, a tunable lens with diodes integrated into the meta-atoms that control the phase profile, resulting in tuning the location of the focal point [30]. Another work in microwave frequency is a beam-steerable metamaterial lens using a varactor diode that controls the beam of the structure by adding a specific set of reverse bias voltages [31]. A frequency-tunable lens-coupled annular-slot antenna (ASA), which works in the G-band between 140-220 GHz, tunes the operation frequency until 50 GHz by controlling the capacitive loading from the varactor [32]. A reconfigurable lens in microwave frequencies for both near- and far-fields has been realized by a non-local metasurface using eight meta-atoms per λ^2 area (λ: wavelength) and varactor diodes where the capacitance can be tuned by an applied bias voltage [33]. Another tunable lens with varactor diodes in the microwave is a holographic meta-mirror to dynamically control the location of the focal point [34]. In [35], a THz metalens is proposed based on graphene surface plasmons, in which the focal length is changed by tuning the Fermi level of electrons in graphene. Another work describes a reconfigurable all-dielectric metalens at a wavelength of 5.2 μm with the ability to switch the focal length between 1.5 and 2 mm by changing the state of $Ge_2Sb_2Se_4Te$ (GSST) [36]. The ability to switch the focal point on and off by controlling the temperature of VO_2has been successfully demonstrated in the THz range [37]. Another example is the efficient all-dielectric metalens based on liquid crystals operating at infrared wavelengths proposed in [38], which provides a 10% variation in focal length. A mechanically reconfigurable metasurface has been shown to be able to

tune focal lengths between 150 and 250 μm at a wavelength of 632.8 nm by changing the lattice of the Au nanorod array on a stretchable polydimethylsiloxane substrate [39]. Another mechanically reconfigurable lens at optical wavelength is a dielectric metasurface based on subwavelength thick silicon nano-bricks encapsulated in a thin transparent elastic polymer, which can tune the focal length between 600 and 1400 μm [40]. Despite these efforts, drawbacks such as complexity and feasibility [35], [36], limitations in tuning the focal length of the lens [37], [38], and mechanical reconfigurability rather than an electrical one are serious obstacles toward the realization of reliable and highly-efficient tunable metalenses [39], [40].

To address these issues, we propose and numerically test a new strategy to achieve a tunable focal length by using a metalens on a ground plane realized with a VO_2 multilayer. The focal length is electrically tuned by changing the effective distance between the metasurface and the ground plane. This novel flat lens, with two VO_2 layers separated by a thermal insulator film and a periodic distribution of silicon bricks, achieves different target phase profiles and can focus millimeter waves at tunable focal points. Compared with previous works on reconfigurable lenses, this structure is easy to fabricate, has an operational speed on the nanosecond order [41], and provides a wide focal length tunability, one of the most challenging properties of tunable lenses.

II. BACKGROUND THEORY AND DESIGN PROCEDURE

The proposed metalens is illustrated in Fig. 1(a)-(c). The structure, designed to provide a tunable focal length at a frequency of 60 GHz (wavelength $\lambda = 5$ mm), is made of silicon bricks distributed periodically in the xy-plane. The bricks sit on top of an ITO film (thickness 100 nm), separated from the copper (Cu) substrate by a VO_2 multilayer buffer. Such a buffer is composed of a bottom VO_2 layer in contact with copper (with a thickness of $h_1 = 0.08$ mm) separated from a top VO_2 layer (with a thickness of $h_2 = 0.12$ mm) by means of a high thermal and electrical insulating layer of Polyvinyl chloride (PVC) foam (see parameters value in Table 1). Both VO_2 layers are much thicker than the skin depth of VO_2 in the millimeter wave in a range of 30 - 300 GHz, which is in the interval 14.81-20.54 μm based on the resistivity data ($2.6 \times 10^{-5} - 5 \times 10^{-4}$ Ω m [42], [43]). The bottom and top VO_2 layer temperatures are independently controlled by an electric current flowing either through the metal at the ground layer or through the thin ITO layer. To prevent the simultaneous thermal switching of both VO_2 layers, a 0.05-mm-thick layer of Polyvinyl chloride (PVC) foam (relative permittivity equal to 2.8) acts as a thermal insulator between the top and bottom VO_2 layers. In this configuration, the device has three possible states (see Fig. 1(d)): The first in which both VO_2 layers have temperatures above $T_c = 68$ °C, and therefore the ground plane is closest to the silicon bricks (we call this state "Metal-Metal"); In the second one, the bottom VO_2 layer has a temperature larger than T_c, and the top one is at a temperature lower than T_c (we name this state "Metal-Insulator"), and therefore the ground plane is at an intermediate distance from the silicon bricks; In the third state, when both VO_2 layers are at low temperatures ("Insulator-Insulator" state), the ground plane is found at the maximum distance from the bricks. It is also possible to set the bottom VO_2 layer to be an insulator and the top one to be metal, but this state is equivalent to the Metal-Metal state since millimeter waves do not reach the bottom layer of VO_2. To summarize, in this structure, the ground plane is located at an electrically tunable distance from the silicon brick's metasurface. The whole system is designed to realize three different phase profiles and, therefore, three different focal distances.

TABLE 1. Parameters value of the proposed structure.

Parameters	Value [mm]	Parameters	Value [mm]
p	2.5	h_1	0.08
a	1.5	h_2	0.12
b	0.1-2.4	h_{ITO}	0.01
h_{Si}	1.7	tm	0.5

To design such a flat lens, the metasurface should provide a phase discontinuity that causes constructive interference at the focal point in front of the structure. For simplicity, we choose a one-dimensional metasurface where the phase distribution along the coordinate x has the following one-dimensional target profile [44], [45], [46]:

$$\phi(x) = \frac{2\pi}{\lambda}\left(\sqrt{x^2 + f^2} - f\right) \tag{1}$$

where λ is the wavelength in vacuum, and f is the focal length of the flat lens.

Using equation (1) as the target phase profile for a given focal distance, the metalenses have been specifically engineered to focalize reflected waves at three distinct focal distances, each corresponding to one of the three system states. In particular, we designed the VO_2 multilayer to have a tunable focal length between 5.4 λ and 6.6 λ, namely, at the three following focal distances: $z_1 = 27$ mm, $z_2 = 31$ mm, and $z_3 = 33$ mm. Thus, based on the data in Fig. 2(a) and (b), the flat lens should provide three target phase profiles using silicon bricks distributed on the supercell in three different states (see Fig. 2(c), (d) and (e)). To calculate the reflection phase as a function of the silicon brick (meta-atom) size (reported in Fig. 2(a)), here we perform full-wave simulations with the finite-difference frequency-domain (FDFD) solver of the CST software. In this simulation, we consider periodic boundary conditions applied to a period with periodicity p containing a single silicon brick and a normally incident plane wave with a linearly polarized electric field in the direction of the x-axis. The relative permittivity of silicon is assumed to be 11.7 [47]. For VO_2, we consider a relative permittivity equal to 9 in the insulting state (below $T_c = 68$ °C) and the frequency-dependent data of [48] for the metal state. The relative permittivity of the foam insulation film, composed of basic Polyvinyl chloride (PVC) material into which air

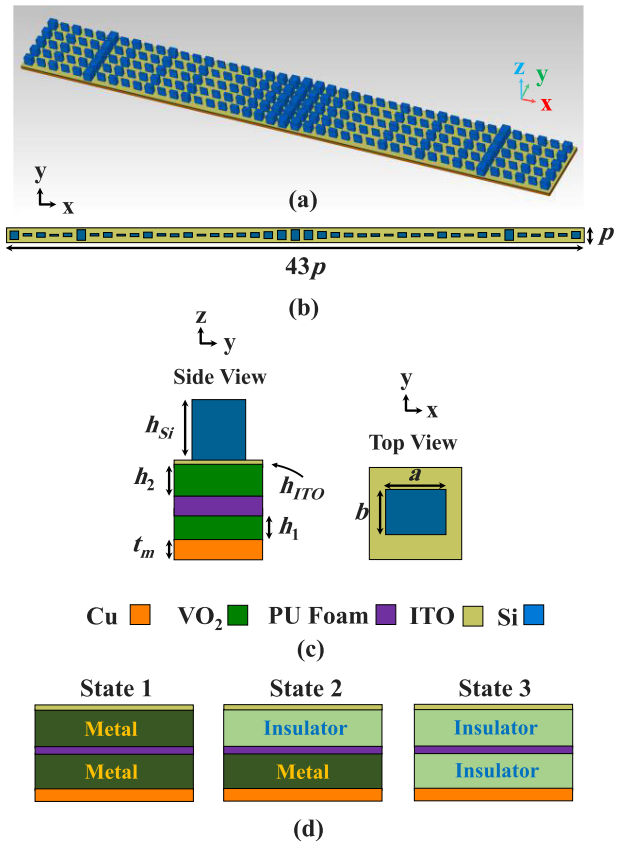

FIGURE 1. (a) Perspective view of the reconfigurable metalens with silicon bricks with a thickness of $h_{Si} = 1.7$ mm. (b) Top view of the supercell of the metalens. (c) The unit cell of the metasurface with the base size of $p = 2.5$ mm and the lateral dimensions a and b, in the direction of the x-axis and y-axis, respectively. The bottom and top VO_2 layers are thermally insulated by Polyvinyl chloride (PVC). The temperature of the VO_2 layers is controlled by an electric current passing through the back metal layer made of copper and the ITO layer. (d) Three different states of the tunable lens due to different combinations of phases in the top and bottom VO_2 layers.

is injected, is set at 2.8 based on experimental data [49]. For the permittivity of copper, the Drude model, fitted to experimental data reported in [50], is adopted. The parameters used in the Drude model of the relative permittivity, $\varepsilon = \varepsilon_\infty - \omega_p^2/(\omega^2 - j\omega\gamma)$, are: $\varepsilon_\infty = 4.68$, plasma frequency $\omega_p = 1.32 \times 10^{15}$ rad/s, and collision frequency $\gamma = 1.05 \times 10^{14}$ Hz. We set the unit cell periodicity, corresponding to a single meta-atom, at $p = 2.5$ mm, which is half of the central wavelength in the bandwidth under investigation. In the numerical analysis, the lateral dimension a of the brick is fixed at 1.5 mm, and the other lateral dimension, b, varies between 0.1 and 2.4 mm. Variations of dimension b produce variations in the phase of the reflected wave that cover the entire range between 0 and 2π, as shown in Fig. 2(a). Using the lookup table data in Fig. 2(a), the sizes of silicon bricks in the supercell, as shown in Fig. 1, were chosen to provide the target phase profiles (see Fig. 2(c)-(e)) required by the flat lens in the three states discussed above. In choosing the brick dimension b, we avoid the Mie resonance visible in Fig. 2(a) for b values near 0.6 mm. This choice prevents

TABLE 2. The lateral dimensions of the silicon bricks meta-atoms are distributed periodically in the supercell of the metalens.

Met	a [mm]	b [mm]	Location on x-axis [mm]
Met1	1.5	1.98	0
Met2	1.5	1.72	- 2.5, +2.5
Met3	1.5	1.28	- 5, +5
Met4	1.5	0.93	- 7.5, +7.5
Met5	1.5	0.72	- 10, +10
Met6	1.5	0.53	- 12.5, +12.5
Met7	1.5	0.42	- 15, +15
Met8	1.5	0.19	- 17.5, +17.5
Met9	1.5	0.88	- 20, +20
Met10	1.5	0.53	-22.5, +22.5
Met11	1.5	0.34	-25, +25
Met12	1.5	1.05	-27.5, +27.5
Met13	1.5	0.54	-30, +30
Met14	1.5	0.30	-32.5, +32.5
Met15	1.5	0.86	-35, +35
Met16	1.5	0.48	-37.5, +37.5
Met17	1.5	1.98	-40, +40
Met18	1.5	0.65	-42.5, +42.5
Met19	1.5	0.33	-45, +45
Met20	1.5	0.83	-47.5, +47.5
Met21	1.5	0.45	-50, +50
Met22	1.5	1.23	-52.5, +52.5

sudden change in the phase profile of the reflection, which may affect the focusing of the reflected wave and guarantees near unity magnitude of the reflection for all the bricks in the supercell and, therefore, improves the focalization capability of the metalens [51]. Due to the low absorption losses in the metallic state of the VO_2 layers, no Ohmic losses within the silicon meta-atoms, and no transmission through the metallic backplane, almost unitary reflectance is achieved.

The key point of the design procedure is the different behavior of the reflection phase in the three different states of the unit cell in Fig. 2(a). As shown in Fig. 2(a), when the distance of the ground plane from the silicon meta-atoms increases, the reflection phase is altered. The amount of this shift changes for different sizes of the silicon brick. This peculiar feature of our design procedure, revealed in Fig. 2(c)-(e), allows us to achieve phase profiles that are very close to the target ones, leading to the possibility of concentrating millimeter waves at different focal distances using different states of the same device.

III. NUMERICAL RESULTS

Next, in this section, we simulate the supercell of the metasurface with the FDFD method using CST. The supercell of a flat metalens consists of 43 meta-atoms, as detailed in Table 2. Periodic boundary conditions are set around the structure at boundaries perpendicular to the x and y axes, and an x-polarized plane wave, with a unitary magnitude electric field, excites the metasurface from the air side. The numerical results are depicted in Figs. 3 and 4.

Fig. 3(a) shows the normalized intensity of the electric field versus the distance from the metalens in the three states. When both VO_2 layers are metallic, the focal point appears at 27 mm from the metasurface, and if the top VO_2 layer

TABLE 3. Features of the previous reconfigurable metalens and the present one in frequency, focal length, its tunability, and the tuning method.

Ref.	Frequency [THz]	Focal Length	Focal Point Displacement	Method of Tuning Focal Length
[35]	5	100 μm	1.6λ	Fermi level of graphene
[36]	57.7	1.5 mm	96λ	Crystallography of GSST
[37]	0.75	3 mm	-	Temperature of VO_2
[38]	193.5	6.25 μm	0.74λ	Liquid crystal
[39]	474	6.25 μm	157λ	Mechanically
[40]	328	1000 μm	874λ	Mechanically
This work	0.06	31 mm	1.2λ	Temperature of VO_2

converts into an insulator (the second state), the focal length becomes 31 mm. Additionally, if both VO_2 layers are in the insulator phase, the focal point is located at the farthest point from the metasurface ($f = 33$ mm). To better clarify the reconfigurable metasurface behavior, the electric field intensity of the reflected wave in the xz-plane is reported in Fig. 3(b)-(d), in which the focal point size in the direction of the x-axis is 2.44 mm, 2.68 mm, and 2.76 mm for states one, two, and three, respectively. Specifically, the focal spot size in different states is about half of the operation wavelength close to the Rayleigh limit. Tuning the temperature of the VO_2 layers controls the location of the focal point. To improve the tunability of the focal length, the number of states in the structure related to the VO_2 layer should be increased to create new phase profiles and focus the reflected wave at different points in front of the flat lens. However, increasing the number of reconfiguring states would increase the complexity of the design in terms of thermal control. The ability to tune the focal length is a key functionality for many applications, including wireless communications.

The other significant feature of this structure is its ability to operate at various frequencies. As proved in previous works on metalenses [44], [52], a frequency increase causes an increase in the focal length. As the frequency becomes lower, the focal point gets closer to the metasurface (see Fig. 4). As can be seen in Fig. 4, changing the frequency leads to a displacement of the focal point. Based on this figure, the range of tunability of the focal length is changed from 25.5-30 mm for a frequency of 58 GHz to 31.5-36 mm for 62 GHz. This feature becomes crucial when some devices operate at a frequency detuned from the target considered in the design procedure. Variations of the focal length induced by frequency shifts can be mitigated by adopting a configuration with more VO_2 layers and, therefore, a larger number of states.

Table 3 summarizes the properties of previous works on different types of reconfigurable metalenses in terms of frequency, amount of focal length displacement, and method. Reference [35] realized a near-field tunable lens in the THz range with a structure and combination of materials (ion-gel and graphene ribbons) that pose several fabrication challenges. In [36], in addition to the considerable complexity of the structure, the focal length can change only between two states at the 5.2 μm wavelength. Another work switches the focal point on and off by controlling the temperature of the VO_2 layer without changing its location [37]. According to [38], the tuning efficiency is about 10% using liquid crystals around silicon resonators, and focal point tuning in [39] and [40] is achieved mechanically. Our tunable metalens

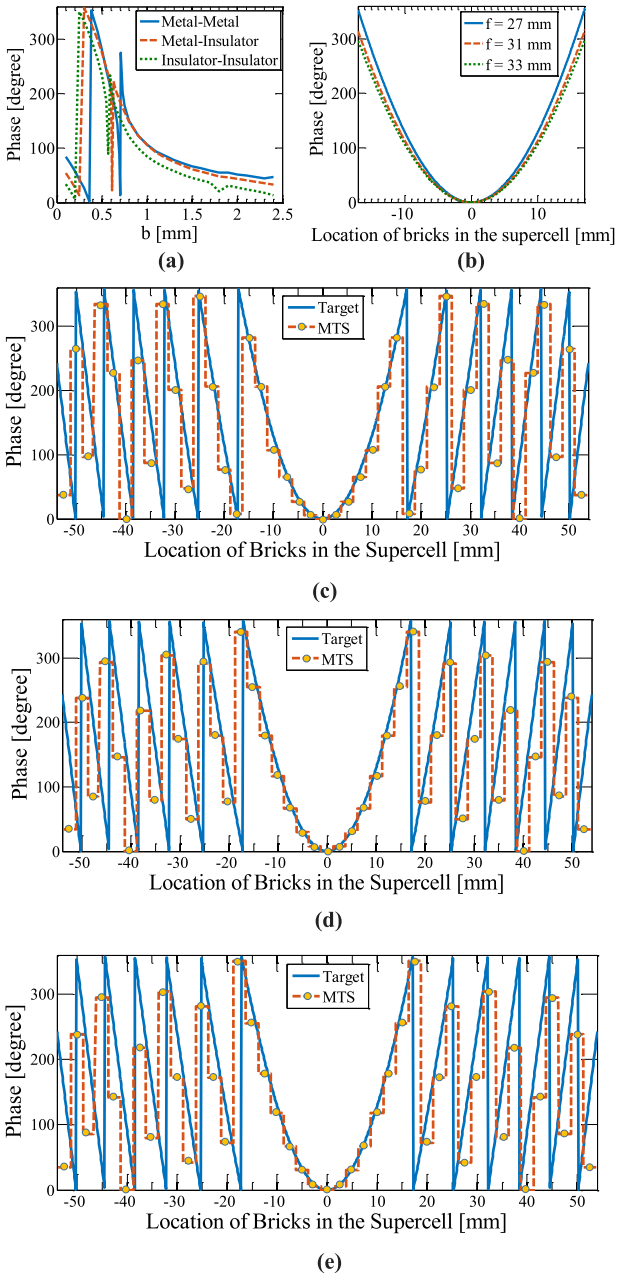

FIGURE 2. (a) The phase of reflection from the unit cell of the metasurface with the periodicity of $p = 2.5$ mm as a function of b, the lateral dimension of the silicon brick, varying in the range of 0.1-2.4 mm, and fixing $a = 1.5$ mm. (b) Target phase profiles of the metalens for tuning the focal length between 27 mm – 33 mm. Target and real phase profiles of reflection for focal lengths of (c) 27 mm, (d) 31 mm, and (e) 33 mm.

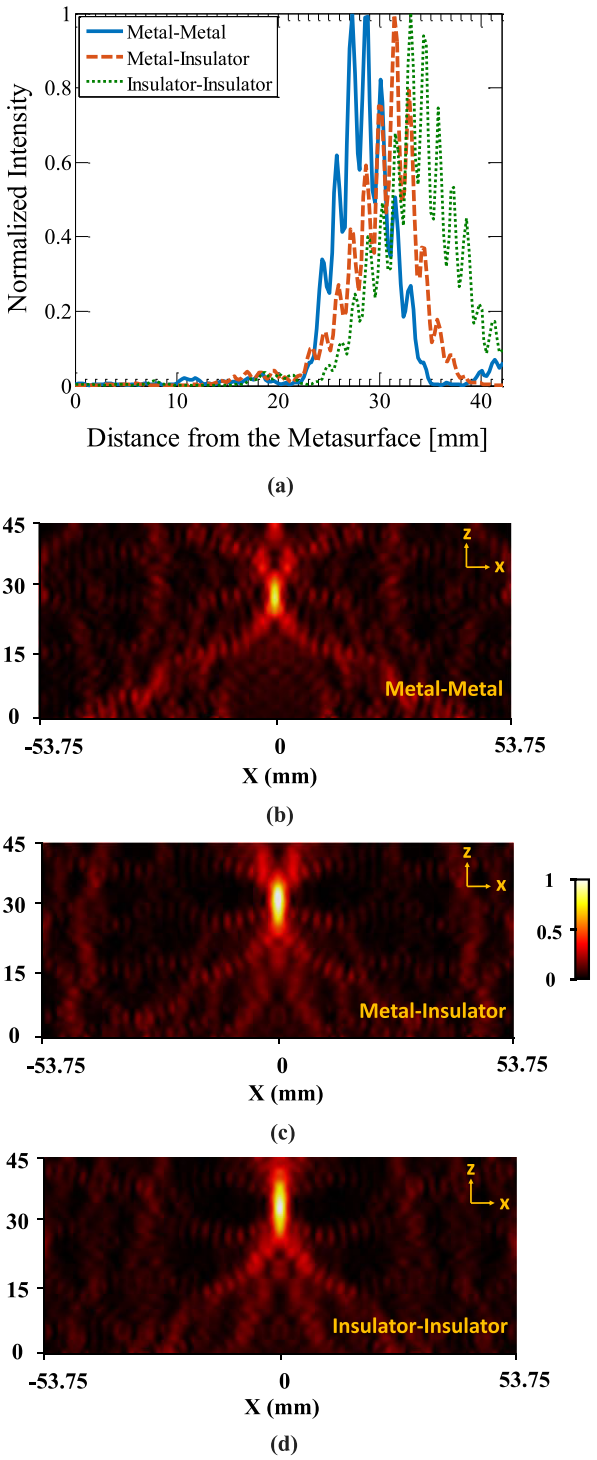

FIGURE 3. (a) The normalized intensity of the total field at 60 GHz along the z-axis for $x = 0$, normalized with respect to the maximum value. The electric field intensity of the reflected field in the xz-plane in the (b) Metal-Metal, (c) Metal-Insulator, and (d) Insulator-Insulator state.

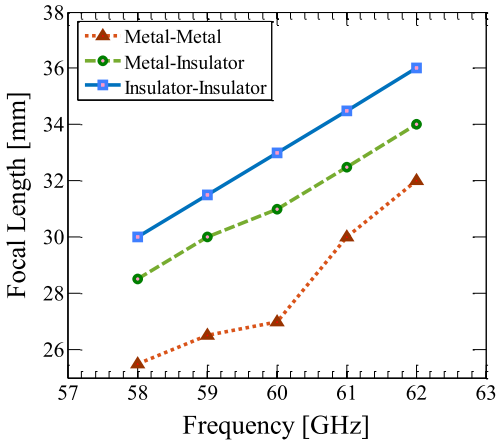

FIGURE 4. The focal length of the tunable metalens versus frequency in states of Metal-Metal, Metal-Insulator, and Insulator-Insulator.

for millimeter waves has a design that allows a relatively simple fabrication process, and it can electrically tune the focal length in the range of 27 - 33 mm (with a tunability range of 1.2 λ and, therefore, an efficiency of about 20%). Moreover, the method proposed in this study can be generalized to tunable metalenses with more than three states so that the focal length may be more accurately controlled. This advantage becomes even more significant when the lens must work in a large operational bandwidth, which is common in communication systems. The tuning abilities of our structure remain virtually unaltered in a relatively large bandwidth in the millimeter wave range. Another advantage of such a method proposed in this paper becomes significant when the metalens is illuminated by off-axis, which is an inevitable problem in wireless applications. In this situation, to control and compensate for the location of the focal point at the focal plane, the resonators should be designed based on $\phi(x) = \frac{2\pi}{\lambda}(\sqrt{(x+\Delta x)^2+f^2}-f)$ in the way that changing the state (temperature of the VO_2 layers) creates an updated phase profile with a revised value of Δx (amount of deviation in the focal plane plan in comparison with the primary situation when $\Delta x = 0$) [35]. In this design, the more phase profiles with different values of Δx, the compensation will be better and more accurate.

The analysis has been performed so far, assuming an infinitely periodic metasurface with the supercell reported in Fig. 1(b) and, therefore, by applying periodic boundary conditions and plane wave excitation. To assess the performance of the metasurface in a more realistic scenario, we investigated the tunability of the focal length when a plane wave illuminates a finite metasurface surrounded by air. In particular, we have considered the structure of Fig. 1(a), with a finite size $43p \times 5p$ in the xy-plane. The values of focal lengths in the three states for the finite structure are in good agreement with those retrieved from the infinitely periodic structure, as summarized in Table 4.

The realization of the proposed structure is compatible with the state of the art [49]. Specifically, the procedure that might be adopted to realize the structure is outlined in the following. The multi-layer structure is composed of a copper layer with a thickness of 0.5 mm on top of which a silicon layer with a thickness of 0.08 mm and a pressed foam are deposited [49]. Next, the top layer of VO_2 and ITO layers shall be added [49]. The metasurface pattern with silicon

TABLE 4. The numerical results of the metalens with infinite periodicity and finite structure.

	FL (MM)	FL (MI)	FL (II)
Periodic	27.3	31.3	33.5
Open	26.8	30.3	32.5

FL: focal length; MM: metal-metal state;

TABLE 5. Thermal properties of the materials used in the thermal simulation of CST.

Material	Density [kg/m^3]	Thermal Conductivity [W/K/m]	Specific Heat [J/K/kg]
Cu	8960	398	385
Si	2329	148	700
VO_2	4570	3.6	690
PVC	1600	0.03	1080
ITO	7140	0.84	341

resonators can be transferred to the photo-resist layer via lithography. After that, through etching, the pattern is created on the supercell of the metasurface. Also, temperature control can be achieved by passing a static electric current through the back metal and ITO layer by using two electrodes at both sides of these regions.

IV. THERMAL INVESTIGATION OF THREE STATES OF THE METALENS

In this section, we investigate the metalens' thermal behavior and how the device's three states are achieved by exploiting different combinations of phases in the two VO_2 layers. To get the results of the previous section, we assumed that two heating mechanisms allow the independent control of the temperature in the two VO_2 layers; namely, an electric current flowing through the copper ground heats the bottom VO_2 layer, bringing its temperature above the critical value T_c, while the electric current passing through the ITO layer under the Si bricks heats up the top VO_2 layer. Thanks to the application of the current in the copper film, the Metal-Insulator state can be reached (top VO_2 layer in the insulator phase and bottom VO_2 layer in the metallic phase). Reaching the Metal-Metal and Insulator-Insulator states is less problematic since, in the absence of currents, the device is obviously in the Insulator-Insulator state. In contrast, the application of both currents induces the Metal-Metal state. Therefore, we have investigated the structure's heat diffusion properties to determine the Metal-Insulator state's existence for a proper application of an electric current flowing in the copper film.

To ascertain this state of operation under thermal steady-state conditions, we solved the heat diffusion equation using the CST software. We set the thermal properties of the materials as in Table 5. Moreover, an open boundary condition with ambient temperature (20 °C) is used for all boundaries, while for the top and bottom boundaries, conduction and radiation heat transfer are enabled in the simulation. The electric current flowing in the copper film heats the whole structure and induces a heat source at the interface with the bottom VO_2 layer, bringing its temperature to 75-102°C ($>T_c$). The thermal simulation results are shown in Fig. 5,

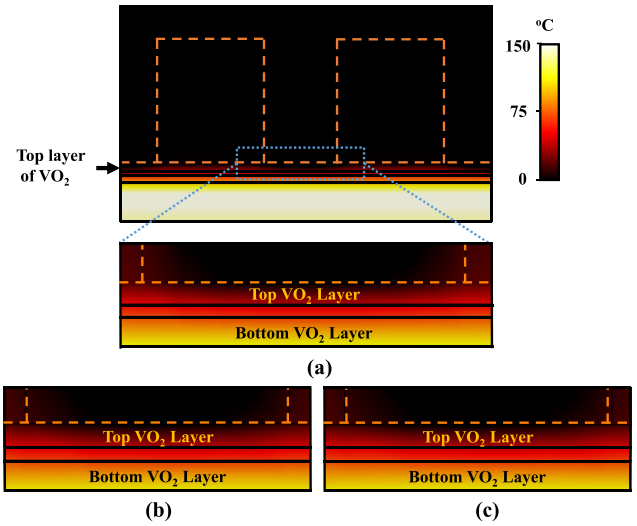

FIGURE 5. Temperature distribution in the *xz*-plane when the heating current is flowing at the interface with copper (the ground metal layer of the structure) (a) based on the thermal properties of materials in Table 5, (b) by increasing and (c) decreasing up to 10% of thermal conductivity of VO_2 and PVC.

where the spatial distribution of temperature is reported in the steady state: the bottom VO_2 layer has a temperature larger than T_c, leading to the transition from the insulator to the metal without any effect on the top VO_2 layer, which remains below T_c, bringing the structure to the desired Metal-Insulator state. In other words, the Polyvinyl chloride (PVC) thermal insulation film inhibits heat propagation and keeps the top VO_2 layer at a temperature lower than T_c, in the insulator state.

Investigating the tunable lens behavior in different temperatures affecting the thermal properties of the materials is a significant step in ensuring the tunability performance of the structure. However, the variation in thermal properties of the Polyvinyl chloride (PVC) layer and thick layers of VO_2 is minor [53], [54] with insignificant impact on the thermal behavior. To verify this claim, we repeat the thermal simulation by increasing and decreasing up to 10% in the thermal conductivity of PVC and VO_2. Based on these simulations, the maximum temperature in the top VO_2 layer changes from 46 °C to 48 °C. Also, the spatial distribution of temperature in both thermal simulations (see Fig. 5 b, c) shows that in the metal-insulation state, the bottom VO_2 layer transits from the insulator to the metal without any effect on the top VO_2 layer, indicating that changing thermal properties of materials in this tunable lens has a no significant impact on the tunability of the structure.

V. CONCLUSION

We presented a new type of metalens with tunable focal length based on integrating a metasurface of silicon bricks with a VO_2-based multilayer. The focal length of the metalens can be electrically tuned by exploiting independent phase transitions in the VO_2 layers. In the proposed configuration, two active layers of VO_2 are separated by an insulating film

to prevent heat conduction between the two VO_2 layers, providing three states of operation corresponding to three different focal lengths. Our numerical investigation results indicate that the proposed metalens' focal length can be tuned between 27 mm and 33 mm at a frequency of 60 GHz. In summary, our concept structure paves the way toward realizing compact devices for millimeter waves with tunable functionalities and activation times in the nanosecond order. We envision applications of tunable metastructures based on VO_2 multilayers in 5G and 6G cellular systems.

REFERENCES

[1] R. W. Heath, N. González-Prelcic, S. Rangan, W. Roh, and A. M. Sayeed, "An overview of signal processing techniques for millimeter wave MIMO systems," *IEEE J. Sel. Topics Signal Process.*, vol. 10, no. 3, pp. 436–453, Apr. 2016.

[2] X. Wang, L. Kong, F. Kong, F. Qiu, M. Xia, S. Arnon, and G. Chen, "Millimeter wave communication: A comprehensive survey," *IEEE Commun. Surveys Tuts.*, vol. 20, no. 3, pp. 1616–1653, 3rd Quart., 2018.

[3] M. Wagih, A. S. Weddell, and S. Beeby, "Millimeter-wave power harvesting: A review," *IEEE Open J. Antennas Propag.*, vol. 1, pp. 560–578, 2020.

[4] U. Gustavsson, P. Frenger, C. Fager, T. Eriksson, H. Zirath, F. Dielacher, C. Studer, A. Pärssinen, R. Correia, J. N. Matos, D. Belo, and N. B. Carvalho, "Implementation challenges and opportunities in beyond-5G and 6G communication," *IEEE J. Microw.*, vol. 1, no. 1, pp. 86–100, Jan. 2021.

[5] D. Moltchanov, E. Sopin, V. Begishev, A. Samuylov, Y. Koucheryavy, and K. Samouylov, "A tutorial on mathematical modeling of 5G/6G millimeter wave and terahertz cellular systems," *IEEE Commun. Surveys Tuts.*, vol. 24, no. 2, pp. 1072–1116, 2nd Quart., 2022.

[6] A. Jawarneh, M. Kadoch, and Z. Albataineh, "Decoupling energy efficient approach for hybrid precoding-based mmWave massive MIMO-NOMA with SWIPT," *IEEE Access*, vol. 10, pp. 28868–28884, 2022.

[7] S. Di Meo, P. F. Espín-López, A. Martellosio, M. Pasian, G. Matrone, M. Bozzi, G. Magenes, A. Mazzanti, L. Perregrini, F. Svelto, P. E. Summers, G. Renne, L. Preda, and M. Bellomi, "On the feasibility of breast cancer imaging systems at millimeter-waves frequencies," *IEEE Trans. Microw. Theory Techn.*, vol. 65, no. 5, pp. 1795–1806, May 2017.

[8] J. E. Johnson, O. Shay, C. Kim, and C. Liao, "Wearable millimeter-wave device for contactless measurement of arterial pulses," *IEEE Trans. Biomed. Circuits Syst.*, vol. 13, no. 6, pp. 1525–1534, Dec. 2019.

[9] M. Barbuto, Z. Hamzavi-Zarghani, M. Longhi, A. Monti, D. Ramaccia, S. Vellucci, A. Toscano, and F. Bilotti, "Metasurfaces 3.0: A new paradigm for enabling smart electromagnetic environments," *IEEE Trans. Antennas Propag.*, vol. 70, no. 10, pp. 8883–8897, Oct. 2022.

[10] E. Basar, M. Di Renzo, J. De Rosny, M. Debbah, M.-S. Alouini, and R. Zhang, "Wireless communications through reconfigurable intelligent surfaces," *IEEE Access*, vol. 7, pp. 116753–116773, 2019.

[11] J. Li, Y. Yuan, G. Yang, Q. Wu, W. Zhang, S. N. Burokur, and K. Zhang, "Hybrid dispersion engineering based on chiral metamirror," *Laser Photon. Rev.*, vol. 17, no. 3, Mar. 2023, Art. no. 2200777.

[12] W. Yang, C. Zhou, Q. Xue, Q. Wen, and W. Che, "Millimeter-wave frequency-reconfigurable metasurface antenna based on vanadium dioxide films," *IEEE Trans. Antennas Propag.*, vol. 69, no. 8, pp. 4359–4369, Aug. 2021.

[13] M. R. M. Hashemi, S.-H. Yang, T. Wang, N. Sepúlveda, and M. Jarrahi, "Electronically-controlled beam-steering through vanadium dioxide metasurfaces," *Sci. Rep.*, vol. 6, no. 1, pp. 1–8, Oct. 2016.

[14] Q. Wang, X. Ge Zhang, H. W. Tian, W. X. Jiang, D. Bao, H. L. Jiang, Z. J. Luo, L. T. Wu, and T. J. Cui, "Millimeter-wave digital coding metasurfaces based on nematic liquid crystals," *Adv. Theor. Simul.*, vol. 2, no. 12, 2019, Art. no. 1900141.

[15] I. B. Mabrouk, M. Al-Hasan, M. Nedil, T. A. Denidni, and A.-R. Sebak, "A novel design of radiation pattern-reconfigurable antenna system for millimeter-wave 5G applications," *IEEE Trans. Antennas Propag.*, vol. 68, no. 4, pp. 2585–2592, Apr. 2020.

[16] Z.-W. Miao, Z.-C. Hao, B.-B. Jin, and Z. N. Chen, "Low-profile 2-D THz airy beam generator using the phase-only reflective metasurface," *IEEE Trans. Antennas Propag.*, vol. 68, no. 3, pp. 1503–1513, Mar. 2020.

[17] P. F. Goldsmith, C-T. Hsieh, G. R. Huguenin, J. Kapitzky, and E. L. Moore, "Focal plane imaging systems for millimeter wavelengths," *IEEE Trans. Microw. Theory Techn.*, vol. 41, no. 10, pp. 1664–1675, Oct. 1993.

[18] H. Yi, S.-W. Qu, B.-J. Chen, X. Bai, K. B. Ng, and C. H. Chan, "Flat terahertz reflective focusing metasurface with scanning ability," *Sci. Rep.*, vol. 7, no. 1, p. 3478, Jun. 2017.

[19] A. Setiawan, A. Yamawaki, N. Yonemoto, H. Nohmi, and H. Murata, "Millimeter-wave imaging using dielectric lens for security application," in *Proc. 19th Eur. Radar Conf. (EuRAD)*, Sep. 2022, pp. 225–228.

[20] M. A. Shameli, M. R. Eskandari, and R. Safian, "Rotational freedom thin-film solar cell using a reconfigurable nano-antenna with 4-Dimethyl-Amino-N-methyl-4-Stilbazolium Tosylate," *IET Optoelectronics*, vol. 16, no. 4, pp. 179–187, Aug. 2022.

[21] M. R. Eskandari, M. A. Shameli, and R. Safian, "Analysis of an electrically reconfigurable metasurface for manipulating polarization of near-infrared light," *J. Opt. Soc. Amer. B*, vol. 39, no. 1, pp. 145–154, 2022.

[22] S. F. Jilani, M. O. Munoz, Q. H. Abbasi, and A. Alomainy, "Millimeter-wave liquid crystal polymer based conformal antenna array for 5G applications," *IEEE Antennas Wireless Propag. Lett.*, vol. 18, no. 1, pp. 84–88, Jan. 2019.

[23] P. Moitra, Y. Wang, X. Liang, L. Lu, A. Poh, T. W. W. Mass, R. E. Simpson, A. I. Kuznetsov, and R. Paniagua-Dominguez, "Programmable wavefront control in the visible spectrum using low-loss chalcogenide phase-change metasurfaces," *Adv. Mater.*, vol. 35, no. 34, Aug. 2023, Art. no. 2205367.

[24] M. Delaney, I. Zeimpekis, D. Lawson, D. W. Hewak, and O. L. Muskens, "A new family of ultralow loss reversible phase-change materials for photonic integrated circuits: Sb_2S_3 and Sb_2Se_3," *Adv. Funct. Mater.*, vol. 30, no. 36, Sep. 2020, Art. no. 2002447.

[25] X. Huang, Z. Liu, Y. Lian, Z.-D. Hu, J. Wu, and J. Wang, "Dynamic beam all-direlectric coding metasurface converter based on phase change materials of GST," *Opt. Laser Technol.*, vol. 159, Apr. 2023, Art. no. 109037.

[26] Y. Li, J. Luo, X. Li, M. Pu, X. Ma, X. Xie, J. Shi, and X. Luo, "Switchable quarter-wave plate and half-wave plate based on phase-change metasurface," *IEEE Photon. J.*, vol. 12, no. 2, pp. 1–10, Apr. 2020.

[27] L. Zhang, X. Q. Chen, S. Liu, Q. Zhang, J. Zhao, J. Y. Dai, G. D. Bai, X. Wan, Q. Cheng, G. Castaldi, V. Galdi, and T. J. Cui, "Space–time-coding digital metasurfaces," *Nature Commun.*, vol. 9, no. 1, p. 4334, Oct. 2018.

[28] S. Savo, Y. Zhou, G. Castaldi, M. Moccia, V. Galdi, S. Ramanathan, and Y. Sato, "Reconfigurable anisotropy and functional transformations with VO_2-based metamaterial electric circuits," *Phys. Rev. B, Condens. Matter*, vol. 91, no. 13, Apr. 2015, Art. no. 134105.

[29] S. Bulja, D. Mirshekar-Syahkal, R. James, S. E. Day, and F. A. Fernández, "Measurement of dielectric properties of nematic liquid crystals at millimeter wavelength," *IEEE Trans. Microw. Theory Techn.*, vol. 58, no. 12, pp. 3493–3501, Dec. 2010.

[30] H. X. Xu, S. Ma, W. Luo, T. Cai, S. Sun, Q. He, and L. Zhou, "Aberration-free and functionality-switchable meta-lenses based on tunable metasurfaces," *Appl. Phys. Lett.*, vol. 109, no. 19, 2016, Art. no. 193506.

[31] Z. N. Wu, W. X. Tang, and T. J. Cui, "A beam-steerable metamaterial lens using varactor diodes," in *IEEE MTT-S Int. Microw. Symp. Dig.*, Jul. 2015, pp. 1–3.

[32] Z. Jiang, S. M. Rahman, J. L. Hesler, P. Fay, and L. Liu, "Design and characterisation of a 200 GHz tunable lens-coupled annular-slot antenna with a 50 GHz tuning range," *IET Microw., Antennas Propag.*, vol. 8, no. 11, pp. 842–848, Aug. 2014.

[33] V. Popov, B. Ratni, S. N. Burokur, and F. Boust, "Non-local reconfigurable sparse metasurface: Efficient near-field and far-field wavefront manipulations," *Adv. Opt. Mater.*, vol. 9, no. 4, Feb. 2021, Art. no. 2001316.

[34] B. Ratni, Z. Wang, K. Zhang, X. Ding, A. de Lustrac, G.-P. Piau, and S. N. Burokur, "Dynamically controlling spatial energy distribution with a holographic metamirror for adaptive focusing," *Phys. Rev. Appl.*, vol. 13, no. 3, Mar. 2020, Art. no. 034006.

[35] W. Yao, L. Tang, J. Wang, C. Ji, X. Wei, and Y. Jiang, "Spectrally and spatially tunable terahertz metasurface lens based on graphene surface plasmons," *IEEE Photon. J.*, vol. 10, no. 4, pp. 1–8, Aug. 2018.

[36] M. Y. Shalaginov, S. An, Y. Zhang, F. Yang, P. Su, V. Liberman, J. B. Chou, C. M. Roberts, M. Kang, C. Rios, Q. Du, C. Fowler, A. Agarwal, K. A. Richardson, C. Rivero-Baleine, H. Zhang, J. Hu, and T. Gu, "Reconfigurable all-dielectric metalens with diffraction-limited performance," *Nature Commun.*, vol. 12, no. 1, p. 1225, Feb. 2021.

[37] J. He, Z. Xie, W. Sun, X. Wang, Y. Ji, S. Wang, Y. Lin, and Y. Zhang, "Terahertz tunable metasurface lens based on vanadium dioxide phase transition," *Plasmonics*, vol. 11, no. 5, pp. 1285–1290, Oct. 2016.

[38] J. Zhong, N. An, N. Yi, M. Zhu, Q. Song, and S. Xiao, "Broadband and tunable-focus flat lens with dielectric metasurface," *Plasmonics*, vol. 11, no. 2, pp. 537–541, Apr. 2016.
[39] H.-S. Ee and R. Agarwal, "Tunable metasurface and flat optical zoom lens on a stretchable substrate," *Nano Lett.*, vol. 16, no. 4, pp. 2818–2823, Apr. 2016.
[40] S. M. Kamali, E. Arbabi, A. Arbabi, Y. Horie, and A. Faraon, "Highly tunable elastic dielectric metasurface lenses," *Laser Photon. Rev.*, vol. 10, no. 6, pp. 1002–1008, Nov. 2016.
[41] Y. Zhou, X. Chen, C. Ko, Z. Yang, C. Mouli, and S. Ramanathan, "Voltage-triggered ultrafast phase transition in vanadium dioxide switches," *IEEE Electron Device Lett.*, vol. 34, no. 2, pp. 220–222, Feb. 2013.
[42] J. Li, W. Yang, D. Chen, Q. Xue, Q. Wen, and W. Che, "Millimeter-wave frequency reconfigurable antenna using simple VO_2-based paired metasurface," *Int. J. RF Microw. Comput.-Aided Eng.*, vol. 32, no. 12, 2022, Art. no. e23454.
[43] H. Kim, N. Charipar, E. Breckenfeld, A. Rosenberg, and A. Piqué, "Active terahertz metamaterials based on the phase transition of VO_2 thin films," *Thin Solid Films*, vol. 596, pp. 45–50, Dec. 2015.
[44] M. A. Shameli and L. Yousefi, "Absorption enhancement in thin-film solar cells using an integrated metasurface lens," *J. Opt. Soc. Amer. B*, vol. 35, no. 2, pp. 223–230, 2018.
[45] F. Aieta, P. Genevet, M. A. Kats, N. Yu, R. Blanchard, Z. Gaburro, and F. Capasso, "Aberration-free ultrathin flat lenses and axicons at telecom wavelengths based on plasmonic metasurfaces," *Nano Lett.*, vol. 12, no. 9, pp. 4932–4936, Sep. 2012.
[46] M. A. Shameli and L. Yousefi, "Polarization-independent dielectric metasurface lens for absorption enhancement in thin solar cells," in *Proc. Bragg Gratings, Photosensitivity Poling Glass Waveguides Mater.*, 2018, Paper no. JTu5A-9.
[47] X. Yang, X. Liu, S. Yu, L. Gan, J. Zhou, and Y. Zeng, "Permittivity of undoped silicon in the millimeter wave range," *Electronics*, vol. 8, no. 8, p. 886, Aug. 2019.
[48] J. Li, Y. Yang, J. Li, Y. Zhang, Z. Zhang, H. Zhao, F. Li, T. Tang, H. Dai, and J. Yao, "All-optical switchable vanadium dioxide integrated coding metasurfaces for wavefront and polarization manipulation of terahertz beams," *Adv. Theory Simul.*, vol. 3, no. 1, Jan. 2020, Art. no. 1900183.
[49] J. Bor, O. Lafond, H. Merlet, P. Le Bars, and M. Himdi, "Technological process to control the foam dielectric constant application to microwave components and antennas," *IEEE Trans. Compon., Packag., Manuf. Technol.*, vol. 4, no. 5, pp. 938–942, May 2014.
[50] Y. V. Stebunov, D. I. Yakubovsky, D. Y. Fedyanin, A. V. Arsenin, and V. S. Volkov, "Superior sensitivity of copper-based plasmonic biosensors," *Langmuir*, vol. 34, no. 15, pp. 4681–4687, Apr. 2018.
[51] C. F. Bohren and D. R. Huffman, *Absorption and Scattering of Light by Small Particles*. Hoboken, NJ, USA: Wiley, 2008.
[52] E. Arbabi, A. Arbabi, S. Kamali, Y. Horie, and A. Faraon, "High efficiency double-wavelength dielectric metasurface lenses with dichroic birefringent meta-atoms," *Opt. Exp.*, vol. 24, no. 16, pp. 18468–18477, 2016.
[53] M. Kok, K. Demirelli, and Y. Aydogdu, "Thermophysical properties of blend of poly (vinyl chloride) with poly (isobornyl acrylate)," *Int. J. Sci. Technol.*, vol. 3, no. 1, pp. 37–42, 2008.
[54] D.-W. Oh, C. Ko, S. Ramanathan, and D. G. Cahill, "Thermal conductivity and dynamic heat capacity across the metal-insulator transition in thin film VO_2," *Appl. Phys. Lett.*, vol. 96, no. 15, Apr. 2010, Art. no. 151906.

MOHAMMAD ALI SHAMELI was born in Isfahan, Iran, in 1993. He received the B.Sc. degree in electrical engineering from the Isfahan University of Technology, in 2015, and the M.Sc. and Ph.D. degrees in the fields and waves of electrical engineering from the University of Tehran, Tehran, Iran, in 2017 and 2021, respectively. He is currently a Postdoctoral Fellow with the University of Padova, Padua, Italy, where he is a member of the Photonics and Electromagnetics Group. His research interests include electromagnetics, photonics, and metamaterials.

MIRKO MAGAROTTO (Member, IEEE) received the M.Sc. degree in aerospace engineering and the Ph.D. degree in science technology and measurements for space from the University of Padova, Padua, Italy, in 2015 and 2019, respectively. He is currently a Research Fellow (RTDa) with the Department of Information Engineering, University of Padua. His current research interests include plasma antennas, plasma numerical simulation, and electric space propulsion.

ANTONIO-D CAPOBIANCO (Member, IEEE) received the B.Sc. degree in electronic engineering and the Ph.D. degree in electronic and telecommunication engineering from the University of Padova, Italy, in 1989 and 1994, respectively. He is currently an Associate Professor with the Department of Information Engineering, University of Padova. His current research interests include theory and numerical modeling in the fields of photonics, plasmonics, and plasma and microwave antennas.

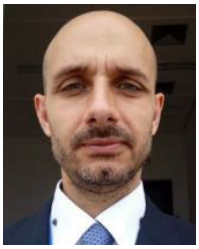

LUCA SCHENATO (Member, IEEE) received the M.Sc. degree in telecommunication engineering and the Ph.D. degree in electronic and telecommunication engineering from the University of Padova, Padua, Italy, in 2003 and 2007, respectively. He is currently an Assistant Professor (RTDb) with the Department of Information Engineering, University of Padova. His current research interests include optical fiber sensors, optical fiber-based devices, and, more recently, metasurfaces and intelligent reflective surfaces.

MARCO SANTAGIUSTINA (Member, IEEE) received the M.Sc. degree in electronic engineering and the Ph.D. degree in electronic and telecommunication engineering from the University of Padova, Padua, Italy, in 1992 and 1996, respectively. He is currently a Full Professor with the Department of Information Engineering, University of Padova. His current research interests include nonlinear optics, optical fibers, and electromagnetic field theory.

DOMENICO DE CEGLIA (IEEE, Member) received the Laurea and Ph.D. degrees in electrical engineering from Politecnico di Bari, Italy, in 2003 and 2007, respectively. He was a Senior Research Associate with the National Research Council, National Academies, USA. He is currently an Associate Professor of electromagnetic fields with the University of Brescia, Italy. He has published more than 100 papers in peer-reviewed journals and proceedings of international conferences in the field of optics and photonics. His research interests include electromagnetics, optics and photonics, with emphasis on plasmonics, light-matter interactions in nanostructures, such as metasurface, metamaterials and nanoresonators, and nonlinear optics.

Open Access funding provided by 'Università degli Studi di Padova' within the CRUI CARE Agreement